

See discussions, stats, and author profiles for this publication at: <https://www.researchgate.net/publication/46254515>

# Gene Silencing Mediated by Magnetic Liposomes Tagged with Small Interfering RNA

ARTICLE *in* NANO LETTERS · OCTOBER 2010

Impact Factor: 13.59 · DOI: 10.1021/nl102485v · Source: PubMed

---

CITATIONS

46

READS

51

## 6 AUTHORS, INCLUDING:



Pablo Del Pino

Philipps University of Marburg

76 PUBLICATIONS 941 CITATIONS

[SEE PROFILE](#)



Dialekti Vlaskou

Technische Universität München

15 PUBLICATIONS 183 CITATIONS

[SEE PROFILE](#)



Pilar Rivera Gil

Universitat Rovira i Virgili & CTQC

105 PUBLICATIONS 3,388 CITATIONS

[SEE PROFILE](#)



Wolfgang J. Parak

Philipps University of Marburg

359 PUBLICATIONS 18,102 CITATIONS

[SEE PROFILE](#)

# Gene Silencing Mediated by Magnetic Liposomes Tagged with Small Interfering RNA

Pablo del Pino,<sup>†,§</sup> Almudena Munoz-Javier,<sup>†</sup> Dialechti Vlaskou,<sup>†</sup> Pilar Rivera Gil,<sup>†</sup> Christian Plank,<sup>\*,†</sup> and Wolfgang J. Parak<sup>\*,†</sup>

<sup>†</sup> Fachbereich Physik und Wissenschaftliches Zentrum für Materialwissenschaften (WZMW), Philipps Universität Marburg, Renthof 7, 35037 Marburg, Germany, and <sup>‡</sup>Institute of Experimental Oncology and Therapy Research, Technische Universität München, Ismaningerstrasse 22, 81675 Munich, Germany

**ABSTRACT** Liposomes made from soy bean oil and a combination of the cationic lipid Metafectene and the helper lipid dioleoylphosphatidyl-ethanolamine were functionalized with magnetic nanoparticles (NPs) and small interfering RNA (siRNA). The resulting magnetic liposomes loaded with siRNA are proven here as efficient nonviral vectors for gene silencing. Embedding magnetic NPs in the shell of liposomes allows for magnetic force-assisted transfection (magnetofection) as well as magnetic targeting in both static and fluidic conditions mimicking the bloodstream.

**KEYWORDS** Magnetic retention, gene therapy, RNA interference, magnetic NPs, delivery, liposomes

Since the original results from Fire, Mello, and co-workers,<sup>1</sup> RNA interference (RNAi) has gained increasing attention due to its remarkable potential to regulate gene expression of virtually any identifiable molecular target. In particular, gene silencing can be induced by small interfering RNA (siRNA), a class of 20–25 nucleotide long double-stranded RNA molecules, through sequence-specific cleavage of perfectly complementary mRNA (mRNA).<sup>2</sup> Despite the promising applications of siRNA-based therapies, so far its use is limited due to the fact that naked siRNA can cross the cellular membrane only under particular conditions due to the limiting strong anionic charge of its phosphate backbone.<sup>3</sup> Additionally, the systemic administration of naked siRNA in vivo is subject to important restrictions like rapid renal clearance following systemic administration due to its small size or rapid degradation by serum and tissue nucleases.<sup>4</sup> Therefore current research efforts are devoted to developing efficient and nontoxic delivery systems which may overcome the intrinsic limitations of naked siRNA delivery.<sup>5–12</sup> These carrier systems are usually classified either as viral or nonviral vectors. Viral vectors show very high transducing efficiency, but their application in humans raises many safety concerns.<sup>13</sup> On the other hand, nonviral vectors represent an attractive alternative which, although being less efficient, are considered safer in handling and for patients, as they do not elicit specific immune responses and are less costly in production.<sup>14</sup>

A wide variety of nonviral vectors have been proposed to shuttle siRNA into cells including cationic lipids,<sup>15</sup> polymers,<sup>16</sup> dendrimers,<sup>17</sup> liposomes,<sup>18</sup> peptides,<sup>19</sup> aptamers,<sup>20</sup> nanoparticles,<sup>21</sup> and complexes combining some of the aforementioned.<sup>22</sup> Nevertheless, many challenges remain to be overcome, such as ease of production, low stability in physiological fluids, or the lack of target specificity.

Coupling magnetic NPs to vectors and carrying out nucleic acid delivery under the influence of a magnetic field gradient (magnetofection) can greatly improve transfection rates due to local accumulation of the vector.<sup>23–25</sup> When designing a magnetic vector for *in vivo* applications, it is critical to take into account the hydrodynamic forces in the bloodstream. There are two routes to optimize magnetic responsiveness of magnetic carriers, either by scaling up the diameter of the magnetic vectors, typically ending up in the micrometer range or by tagging the vector with a number of small NPs to sum up all their magnetic moments.

Herein, we propose liposomes loaded with magnetic NPs and siRNA as a nonviral vector for siRNA delivery into cells under conditions mimicking the bloodstream. Our magnetic vector is based on the formulation previously proposed by Unger and co-workers.<sup>26</sup> Originally Unger's formulation was designed for ultrasound mediated delivery of lipophilic drugs. We on purpose deviated from Unger's formulation in order to functionalize acoustically active liposomes (AALs) with magnetic NPs and siRNA molecules to form magnetic acoustically active liposomes tagged with siRNA (MAALs/siRNA). Briefly, soy bean oil forms the basis of the liposomes and is stabilized with a combination of a cationic lipid, Metafectene (Biontex, Germany), and the helper-lipid dioleoylphosphatidyl-ethanolamine (DOPE) (Avan-

\* Corresponding authors, plank@lrz.tu-muenchen.de and wolfgang.parak@physik.uni-marburg.de.

§ Present address: Instituto de Nanociencia de Aragon (INA), Universidad de Zaragoza, Spain.

Received for review: 05/9/2010

Published on Web: 09/13/2010

ti Polar Lipids). Metafectene is a gene transfer reagent usually used to compact DNA/RNA and facilitate its entry into cells.<sup>28</sup> In our formulation, Metafectene is required to accommodate nucleic acids. DOPE improves transfection relative to that obtained with cationic lipids alone.<sup>29</sup> A number of functions have been proposed for DOPE such as playing a role in fusion of the lipidic complex/lipids with the cellular membrane or weakening the intensity of the charge interaction between DNA and the cationic amphiphile, thereby eventually promoting an effective dissociation of DNA from the complex.<sup>30</sup> In order to confer magnetic responsiveness to the lipospheres, we added to the preparation magnetic nanoparticles.

In a recent work, we have characterized the physical and chemical properties of the MAAL/siRNA system as we use it here.<sup>27</sup> In the work presented here the fate of MAAL/siRNA upon cellular uptake is investigated *in vitro*. First, the efficiency and cytotoxicity of magnetic lipospheres upon cellular ingestion is investigated in cellular cultures. Transfection efficiency is assayed by a 96-well format screening procedure previously reported for magnetic lipidic complexes carrying siRNA.<sup>31</sup> Second, the uptake mechanism is studied by confocal microscopy. And third, under fluidic conditions mimicking the bloodstream, magnetofection efficiency of MAALs/siRNA to down-regulate enhanced green fluorescence protein (eGFP) gene expression in GFP-transfected cells is assessed by fluorescence microscopy. This allows for characterizing drug delivery and optimizing delivery systems before going into animal models. In this manner it serves the objectives of the three R's principle (replacement, reduction, refinement [of animal experiments]).

**Results and Discussion.** The major goal of this study was to find out whether MAALs/siRNA can efficiently deliver siRNA into living cells and in case this was true, to which extent they can interfere with the expression of two gene reporters, firefly luciferase (fLuc) and enhanced green fluorescent protein (eGFP). In order to achieve high magnetofection efficiency, we needed optimal magnetic formulations, and therefore, the incorporation of different magnetic NPs, varying mainly in the coating/stabilizing agent, had to be tested. Magnetic iron oxide NPs coated with the nonionic surfactant Tween 60 (chemicell GmbH, Berlin, Germany) proved to be a good candidate in terms of stability, and as a large number of them could be incorporated in the liposphere shell, magnetic retention could be improved. Other magnetic iron oxide NPs could not be incorporated into the liposphere shell or resulted either in unstable formulations or unable to gene silencing (Supporting Information, section I, Incorporation of Magnetic NPs to Lipospheres). It is also crucial to choose a balanced formulation in terms of stability. MAALs/siRNA have to be able to deliver siRNA into the cytosol of cells upon uptake, and formulations leading to a very rigid constituency might impair siRNA delivery. Empirically, we found as most suitable formulation a 3.4:1 molar

ratio of DOPE (3.6 mM) to Metafectene (1.06 mM), 1 mg of Tween 60-coated magnetic NPs (dry weight), and 50  $\mu$ g (3.1 nmol) of siRNA per mL of MAAL suspension, with 5% v/v of soy bean oil.

The lipid shell of the structure could be visualized by fluorescence microscopy by using a fluorescence labeled lipid as can be seen in the Supporting Information (Figure SI-2(A)). Magnetic NPs were proven to be tightly associated with the MAAL shell, as no iron could be measured in the supernatant of the MAAL suspension after magnetic sedimentation. The magnetic vectors (MAALs/siRNA) could be loaded with up to 500  $\mu$ g of siRNA per mL of the suspension, with a binding capacity of over 98% when the cationic lipid context of the preparation was scaled-up accordingly. The incorporation of siRNA could be verified with fluorescence-(Supporting Information, Figure SI-2(B)) or radioactive-labeled siRNA upon magnetic sedimentation of MAALs. The lipospheres that contained fluidMAG-Tween-60 nanoparticles had an average diameter of  $4.8 \pm 3.7 \mu\text{m}$  and 94.3% of the magnetic lipospheres loaded with siRNA were found smaller than  $10 \mu\text{m}$  (Supporting Information, Figure SI-2(C)). The magnetic liposphere concentration was determined at  $10^9$  lipospheres per mL of suspension by counting under the optical microscope.

Mykhaylyk and co-workers devised a protocol for screening magnetofection efficiency of magnetic vector formulations in cells of any type cultured in 96-well plates.<sup>32</sup> Here, quantitative evaluation of reporter gene down regulation was achieved in cell culture using HeLa or H441 cells stably transduced with fLuc or eGFP reporter genes (fLuc-HeLa, eGFP-HeLa, and eGFP-H441 cells), by measuring the luminescence and/or fluorescence units of protein expressed in the corresponding cell lysates per weight of total protein normalized to the reference (untreated) cells (Figure 1). The cells were exposed to MAALs/siRNA with a concentration of siRNA ranging from 4 to 64 nM using a permanent magnetic plate of 130–240 mT and a magnetic field gradient of 70–120 T m<sup>-1</sup>, which was placed under the cell culture plate for 30 min. To account for cytotoxicity effects, the respiration activity of the cells was analyzed by a test based on 3-(4,5-dimethylthiazol-2-yl)-2,5-diphenyltetrazolium (MTT) as shown in Figure 1.<sup>31</sup>

As shown in Figure 1, upper panels, in eGFP-H441 bronchial epithelial cells at 48 h post-transfection, we measured up to about 60% down-regulation of eGFP gene expression with increasing concentrations of siRNA against eGFP up to 64 nM. In this case, the cell viability is not significantly affected; we do not find a clear dose response tendency to state that increasing concentrations of siRNA correspond to increased cell death. Also, the application of ultrasound does not appear to have any relevant effect on cell viability or silencing efficiency. In eGFP-HeLa cells, middle panels, we reached up to 90% down regulation of eGFP gene expression while cell viability was only slightly compromised at high concentrations of siRNA and with

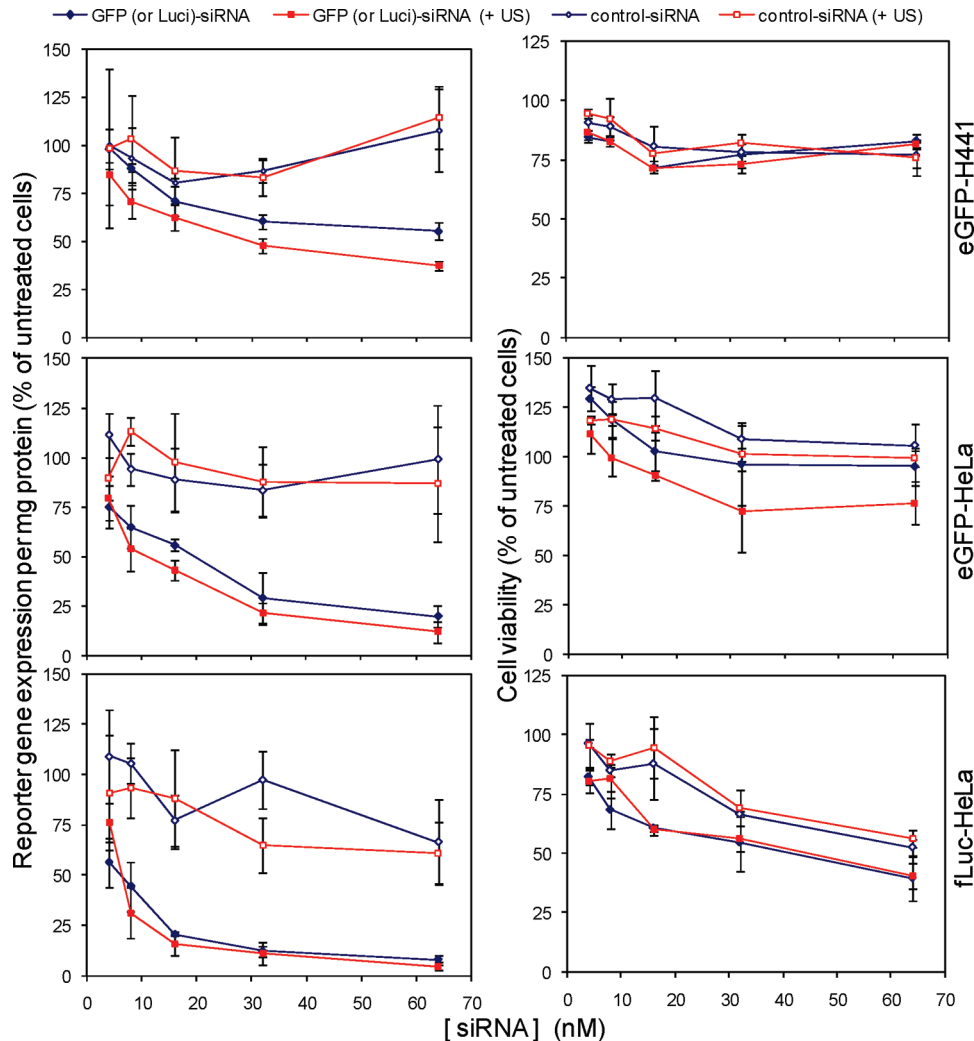


**FIGURE 1.** Down regulation of eGFP and fLuc gene expression referenced to untreated cells with magnetic acoustically active lipospheres loaded with siRNA against eGFP (GFP-siRNA) or fLuc gene (Luc-siRNA) 48 h postmagnetofection. The transfection was carried out in eGFP-H441 bronchial epithelial cells (upper left diagram), in eGFP-HeLa cervical cancer cells (center left diagram), and in fLuc-HeLa (bottom left diagram, data taken from Vlaskou et al.<sup>27</sup>) in the absence and presence of ultrasound (+US). Ultrasound was applied using a Sonitron 2000D device operating at 1 MHz and using a 3 mm ultrasound probe operating at  $2 \text{ W cm}^{-2}$  and a 50% duty cycle for 30 s. The transfection efficiency diagrams are accompanying with corresponding cell viability diagrams (MTT-toxicity assay) on the right side. In all experiments MAALs/siRNA loaded with negative control siRNA, i.e., siRNA with random sequence, is included. Error bars represent standard deviation.

ultrasound application; it should be noted however that in this particular case, the standard deviation of these data is very high. In fLuc-HeLa cells, where the cell viability was already reduced to about 50% after transfection with concentrations of 16–64 nM siRNA, we found an absolute value of down regulation of fLuc gene expression of about 90%. Both the siRNA against the fLuc gene and the corresponding random siRNA controls show an increased cell death tendency corresponding to increasing siRNA doses in HeLa cells. This fact allows us to speculate that this effect is due to the toxicity of the siRNA directed against fLuc in this particular cell line. Interestingly, the same delivery system in the same cell line with siRNA directed against eGFP was rather nontoxic. Hence, we conclude that the observed toxicity in fLuc-HeLa cannot be attributed to components of the delivery system alone. It is known that siRNAs can

activate the innate immune system, being a potent inducer of type I interferon alpha (IFN- $\alpha$ ).<sup>33</sup> Additionally, cationic lipids used as vectors for siRNA delivery are known to have unspecific cytotoxic effects.<sup>34</sup> And finally, high concentrations of siRNA can have cytotoxic effects by oversaturation of cellular pathways of RNA interference.<sup>35</sup>

We want to emphasize the fact that the application of the MAALs/siRNA in cell culture achieved a down regulation of reporter gene expression at low concentrations of 8–16 nM siRNA, even at 4 nM siRNA, particularly in HeLa fLuc and HeLa eGFP cells. The results show a high percentage of knockdown of reporter gene expression, which is dependent on siRNA-concentration loaded on MAALs, even after consideration of the cell toxicity results of the MTT-assay. Additional cytotoxicity data can be found in the Supporting Information (section III, Cytotoxicity Additional Data).

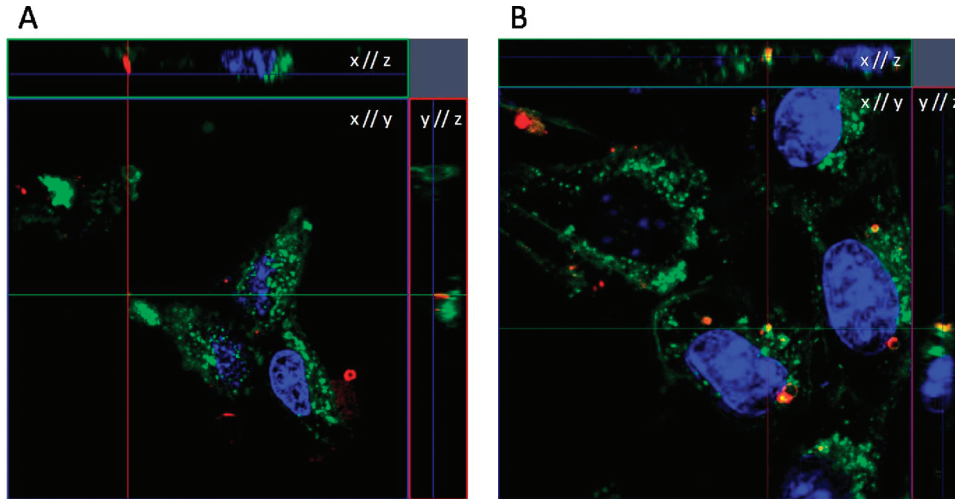


**FIGURE 2.** Intracellular uptake of magnetic acoustically active liposomes with rhodamine-labeled siRNA (MAALs/siRNA<sup>Rh</sup>). 3T3/NIH fibroblasts were incubated with MAALs/siRNA<sup>Rh</sup> (red color of the rhodamine label) and images were taken on living cells over time with a confocal laser scanning microscope (A) immediately after addition and (B) after 60 h of incubation. Hereby the nucleus and cellular membrane of the living cells had been stained in blue with DAPI and in green with WGA488, respectively, directly before imaging. An orthogonal view of the localization of MAALs/siRNA<sup>Rh</sup> in the cells from different planes ( $x//y$ ,  $x//z$ , and  $y//z$ ) is shown. Immediately after addition of MAALs/siRNA<sup>Rh</sup>, most of the liposomes were located extracellularly. However, even at this early time point, some were already found to be sitting on the cell membrane (see cross sections  $y//z$  and  $x//z$ ). After 60 h, there was a notable accumulation of MAALs/siRNA<sup>Rh</sup> inside the cells.

When we exposed the MAAL preparation and the cells to 1 MHz ultrasound in combination with a permanent magnetic field, we also found a high degree of reporter gene down regulation as shown in Figure 1. This cannot be accounted for by cell toxicity due to the ultrasound as was confirmed by the preserved viability of the negative control (MAALs loaded with negative control siRNA). On comparisons of the results in the absence and presence of ultrasound, a slight difference on gene expression was observed when ultrasound was applied. However at the same time, ultrasound application resulted in slightly higher cell toxicity. We know from previous work that MAALs do not respond to ultrasound to an extent like ultrasound microbubbles used as ultrasound contrast agents.<sup>27</sup> MAALs are based on a formulation first developed by Unger et al. for the delivery of hydrophobic drugs.<sup>26</sup> Only a fraction of it get destroyed when applying the ultrasound settings of the Sonitron 2000D device which was used in our study. Hence, under these settings MAALs are less suitable for sonoporation than classical ultrasound microbubbles. On the other hand, MAALs offer the opportunity of magnetic targeting under flow conditions. Therefore further investigation of the siRNA internalization in cells and transfection of cells with MAALs/siRNA were carried out without the application of ultrasound but under settings of magnetic targeting under flow conditions.

By using confocal laser scanning microscopy, we visualized the pathway by which siRNA loaded into MAALs is released into the cytosol and reaches its target. NIH-3T3 embryonic mouse fibroblasts were incubated with MAALs complexed with rhodamine-labeled siRNA (MAALs/siRNA<sup>Rh</sup>) and images of the cells were taken after different incubation times. As expected, immediately after addition of the MAALs/siRNA<sup>Rh</sup>, they are found extracellularly (Figure 2A). Interest-

ingly, even at this early point an accumulation on the cell membrane is already visible (Supporting Information, Figure SI-4(A)). This is likely to be due to the effect of the permanent magnetic field applied to the cells that quickly brings the liposomes into close contact with the cell membrane. Live cell imaging (Supporting Information, Figure SI-4(A)) confirmed internalization of the MAALs/siRNA<sup>Rh</sup>. Internalized liposomes appeared structurally intact. After 60 h (Figure 2B), almost all the liposomes carrying the rhodamine-labeled siRNA were located inside the cells. In order to avoid possible artifacts, z-scans were performed to distinguish between intracellularly and extracellularly located MAALs/siRNA<sup>Rh</sup> (Supporting Information, Figure SI-4(B)). Additionally, images of the internalized MAALs/siRNA<sup>Rh</sup> were taken from different planes to confirm their localization (Supporting Information, Figure SI-4(C)). For sake of clarity on how uptake was optically confirmed, images of noninternalized but membrane-bound liposomes after 60 h are also shown (Supporting Information, Figure SI-4(C)). As a first step during cellular uptake, the magnetic force gradient surely causes local accumulation of the magnetic liposomes at the outer membrane of the target cells, which we already demonstrated in a similar system before.<sup>36</sup> To account for the further internalization of MAALs/siRNA, three different scenarios seem possible. In a first scenario one could think that the force of the magnetic field gradient acting on the liposomes might be able to directly pull the liposomes across the cell membrane into the cytosol and subsequently siRNA would be released either because of cellular degradation of the liposomes or because of their mechanical stability. In a second scenario the liposomes might fuse with the lipidic components of the cellular membrane and thereby would release siRNA to the cytosol. Third, lipo-

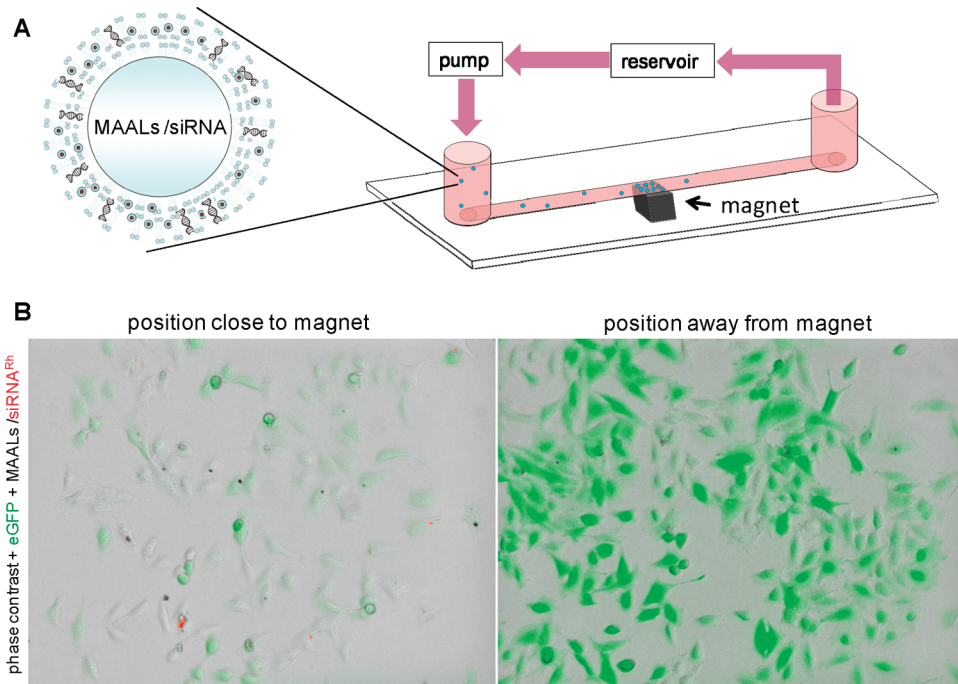


**FIGURE 3.** Magnetofection under fluidic conditions: (A) sketch of the model system used for the magnetofection experiments using MAALs/siRNA<sup>Rh</sup>; (B) optical microscopy images taken 72 h after magnetofection. The images represent the phase contrast image merged with green (eGFP) and red (siRNA<sup>Rh</sup>) fluorescence images of eGFP transfected HeLa cells which are cultivated in a flow channel. Left panel: image of cells at a position close to a magnet which had been placed under the flow channel. Right panel: image of cells at a position far away from the magnet.

spheres might be endocytosed, degraded in the endosome and subsequently released from there to the cytosol. We have to clearly state that our experimental data do not allow for claiming one of the suggested pathways. However, based on findings of similar systems,<sup>6</sup> we speculate that the last scenario takes place. Data shown in Figure 2 would be also compatible with this scenario, as the finding of intact liposomes inside membrane-surrounded intracellular compartments suggests an endocytosis-like mechanism. Summarizing, the application of an external inhomogeneous magnetic field allows liposomes to come in close proximity with the cells. We then speculate that after their internalization via endocytosis-like processes and due to the presence of DOPE, the liposomes lose stability, and the siRNA can exit the compartments.

Figure 3A shows the model flow channel system used in our experiments, which was adopted from a previous study.<sup>36</sup> MAALs/siRNA<sup>Rh</sup> were injected into a reservoir containing cell medium which was connected to a flow channel (ibidi Integrated Biagnostics, Martinsried, Germany) through a peristaltic pump. The velocity of the flow was regulated by the pump and set at  $16 \text{ cm s}^{-1}$ . This value was chosen to be comparable to the blood flow rates in major arteries. Overnight eGFP-HeLa cells were grown on a surface area of  $250 \text{ mm}^2$ . A cubic permanent magnet (NbFeB, 5 mm edge length, magnetic field strength of 1.3 T) was placed under the flow channel for 1 h while the medium was running. After removal of the magnet, we exchanged the reservoir solution for fresh medium in order to remove

liposomes which were not taken up by the cells. The chamber was then stored in an incubator for further analysis at different times of incubation by fluorescence microscopy (after 48 and 72 h, Supporting Information, Figures SI-5.1(A) and (B), Figures SI-5.2(A) and (B), and Figures SI-5.3(A) and (B)). Data show that eGFP-expression was greatly down regulated, as can be observed for example in Figure 3(B) by simple visual inspection. These results demonstrate that by means of magnetic-force, MAALs can efficiently deliver siRNA into cells in a functional form even under fluidic conditions mimicking the circulatory system. This fact suggests that they might be a suitable system for gene delivery *in vivo*.

In this study, magnetic liposomes have been proven to be an excellent candidate as nonviral vector for siRNA delivery. We show that choosing balanced formulations in terms of stability/electrostatic interactions for these hybrid structures can make them very versatile for functional delivery of siRNA into the cytosol of cells. These customized magnetic liposomes show good stability in fluidic conditions mimicking the circulatory system in which magnetic retention was greatly achieved at desired places by exerting a gradient magnetic field. In literature several studies can be found in which magnetofection has been proven to greatly enhance gene transfection efficiency compared to other approaches using nonmagnetic vectors.<sup>24,25,31,32</sup> Also under flow conditions, siRNA can be magnetically targeted AND is active in gene silencing. This can be essential in several envisaged applications of siRNA or gene therapy such

as delivery to tumor-feeding blood vessels or in cardiovascular indications (enforcing or silencing neo-angiogenesis, or restenosis, or silencing inflammatory reactions) or in organ transplantation (silencing graft versus host reactions) or in tissue engineering (directing localized cell differentiation). Although the system discussed in this work does not represent *per se* an improvement in terms of efficiency of siRNA delivery, our system offers an additional feature: magnetic accumulation of the carriers in fluidic conditions mimicking the bloodstream. To our opinion magnetic liposomes have promising potential for *in vivo* applications.

**Experimental Section. Reagents.** Iron oxide nanoparticles coated with Tween 60 (fluidMAG-Tween 60; 90 mg/mL in water) were kindly provided by Christian Bergemann (chemicell GmbH, Berlin, Germany) and have been described in a recent study.<sup>27</sup> DOPE (1,2-dioleoyl-sn-glycero-3-phosphoethanolamine) was purchased from Avanti Polar lipids (Alabaster, AL). Metafectene, the cationic lipid being, apart from soybean oil, the major component of the magnetic liposomes was kindly provided by Biontex GmbH (Martinsried, Germany). The following siRNA duplexes were used: green fluorescent protein (GFP) siRNA duplex (catalog no. D-001300-01-20) and negative control-siRNA, siGENOME Non-Targeting siRNA #1 (catalog no. D-001210-01) were obtained from Dharmacon (Lafayette, USA). Luciferase GL3-siRNA (catalog no. 10220073) and GFP 22 siRNA Rhodamine (catalog no. 1022178) were purchased from Qiagen (Hilden, Germany). Labeled and nonlabeled siRNA duplexes against firefly luciferase, eGFP and control siRNA duplexes were reconstituted with siRNA suspension buffer at a final concentration of 20  $\mu$ M and stored in aliquots at -20 °C. Soybean oil was provided by the hospital pharmacy (Klinikum rechts der Isar, Technical University of Munich).

**Preparation of MAALs/siRNA.** Briefly, a lipid stock solution containing Metafectene (1.06 mM) and DOPE (3.6 mM) was prepared in buffer (NaCl 0.9 % w/v—glycerol—propylene glycol in 8:1:1 v/v). In a microcentrifuge tube, 11.1  $\mu$ L of the stock of fluidMAG-Tween 60 magnetic NPs (90 mg/mL) was mixed with 90.5  $\mu$ L of the lipid stock solution. The mixture was diluted to 1 mL with buffer. Then 2.87 nmol ( $\approx$ 40  $\mu$ g) siRNA from a 20  $\mu$ M siRNA stock solution was added to the mixture and mixed well. The mixture was pipetted in a 2 mL Wheaton vial (Wheaton, Millville, NJ), where soy bean oil had been already pipetted in to have a concentration in the final solution of 5 % v/v, and sealed with an aluminum sealing cap (Wheaton). The headspace of the vial was filled with perfluoropropane gas (C<sub>3</sub>F<sub>8</sub>) (Linde AG, Höllriegelskreuth, Germany), and the vial was shaken for 60 s at 2500 rpm using a Mini BeadBeater (Biospec Products Inc., Bartlesville, OK).

Additionally, for the flow experiments and confocal microscopy, MAALs were prepared as previously stated but with rhodamine-labeled siRNA (GFP-22 siRNA, Rhodamine; Qiagen, catalog no. 1022176).

**Fluorescence Labeled MAALs.** These were prepared either using DiOC18: (3,3'-dioctadecyloxacarbocyanine perchlorate) as a lipophilic tracer from Molecular Probes (Eugene, OR) (484/501 nm) to stain the lipid stock solution (12  $\mu$ g of DiO per mg lipid added to the lipid stock solution) or using rhodamine-labeled GFP-22 siRNA (Qiagen, catalog no. 1022176;  $\lambda_{\text{ex}} = 550 \text{ nm}$ / $\lambda_{\text{em}} = 570 \text{ nm}$ ).

**Characterization of MAALs.** MAAL concentration was determined by the electrical sensing zone-method using a Z2 Coulter counter (Beckman Coulter GmbH, Krefeld, Germany). The size was determined by an image analysis program developed for our magnetic vectors by S.CO Life-Science GmbH (Garching, Germany). Hereby for each sample, after dilution of 5  $\mu$ L of MAAL in 2 mL of PBS (phosphate buffered saline) and magnetic sedimentation in a 24-well plate, 10 representative microscopy images (fluorescence or phase contrast) were analyzed.

**Binding Capacity of siRNA to MAALs.** The quantitative incorporation of siRNA into the magnetic liposomes was confirmed by fluorescence microscopy after preparation of MAALs loaded with 50, 250, and 500  $\mu$ g of rhodamine-labeled siRNA per mL of preparation and determination of the fluorescence ( $\lambda_{\text{ex}} = 485 \text{ nm}$ / $\lambda_{\text{em}} = 560 \text{ nm}$ ) in 100  $\mu$ L aliquots of the supernatant after magnetic sedimentation using a Wallac Victor 2 Multilabel Counter (PerkinElmer). A standard curve was obtained from 100  $\mu$ L samples of a dilution series in water of rhodamine labeled siRNA. Double-distilled water (ddH<sub>2</sub>O) was used as blank.

**Cellular Transfection with siRNA-Loaded MAALs.** For this purpose, HeLa cells (human cervical epithelial adenocarcinoma cells) and NCI-H441 human pulmonary epithelial (H441) cells derived from papillary carcinoma of lungs were used, which were stably expressing the firefly luciferase and/or the eGFP gene obtained upon retro- or lentiviral transduction. Cells were cultured in Dulbecco's modified Eagle medium (DMEM) and in modified RPMI 1640 medium, respectively, supplemented with additives and incubated at 37 °C in 5 % CO<sub>2</sub> atmosphere. Transfection studies for luciferase knockdown were performed using Luci GL3 siRNA (QIAGEN GmbH, Hilden, Germany) and as negative control siRNA a GFP 22 siRNA duplex (Dharmacon, Bonn, Germany). Studies for eGFP knockdown were performed using a GFP 22 siRNA duplex and as negative control a control siRNA (Dharmacon). Before transfection, 7  $\times$  10<sup>5</sup> HeLa fLuciferase, 7  $\times$  10<sup>5</sup> HeLa eGFP, and 2.5  $\times$  10<sup>4</sup> H441 eGFP cells were seeded into the wells of 96-well dishes. One hundred microliters of MAAL/siRNA corresponding to siRNA doses of 4, 8, 16, 32, and 64 nM were added to individual wells, respectively. The total volume was 250  $\mu$ L/well. During the transfection procedure, culture plates were either positioned on a magnetic plate or kept in the absence of a magnetic field. A magnetic field of 130–240 mT and a field gradient of 70–120 T·m<sup>-1</sup> were applied using 96-Magnets Magnetic Plate (OZ Biosciences, France). After 15 min of incubation, ultrasound at 2 W cm<sup>-2</sup> was applied to selected

wells for 30 s with duty cycles set to 50 %. For this purpose, a 3 mm ultrasound probe of a Sonitron 2000 D ultrasound source (Rich Mar Inc., Inola, OK) was inserted directly into the medium covering the cells with the lower end of the source remaining positioned about 4 mm above the culture plate bottom covered by the adherently growing cells. After ultrasound exposure, the culture plate under magnetic field influence remained positioned on the magnetic plate for another 15 min at room temperature. Then, the magnetic plate was removed and the medium was replaced in all wells with fresh complete medium with all additives. Forty eight hours post-transfection, the respective assays for detection of reporter gene expression and protein content were performed. Cell viability was evaluated in terms of cell respiration activity using the MTT-based assay according to previous work.<sup>31</sup>

**Confocal Microscopy.** The fluorophores DAPI-dilactate ( $\lambda_{\text{ex}} = 405 \text{ nm}$  and  $\lambda_{\text{em}} = 460 \text{ nm}$ ) and Wheat Germ Agglutinin-Alexa 488 (WGA488) ( $\lambda_{\text{ex}} = 488 \text{ nm}$  and  $\lambda_{\text{em}} = 519 \text{ nm}$ ) were purchased from Molecular Probes. Living cells were seeded at a concentration of  $2 \times 10^4$  cells/chamber in 300  $\mu\text{L}$  growth medium (DMEM-F12 Ham's supplemented with 10% calf serum, 1% L-glutamin, and 1% penicillin/streptomycin) in an Ibidi-plate and were incubated with MAALs/siRNA<sup>Rh</sup> at a final siRNA concentration of 64 nM. Immediately after addition, the plate was incubated above a permanent magnet (NbFeB, 5 mm edge length, magnetic field strength of 1.3 T) for 20 min to target the magnetic liposomes to the cells. Cells were then either immediately imaged ( $t = 0 \text{ h}$ ) or further incubated at 37 °C 5% CO<sub>2</sub> for different periods of time. Immediately before imaging, the membranes of the cells were stained with WGA488 (60  $\mu\text{g} \cdot \text{mL}^{-1}$ ) for 30 min at room temperature. During the last 5 min DAPI was also added (1  $\mu\text{M}$ ) to the solution to allow for nuclear staining. After 30 min total incubation time, cells were washed three times with PBS and were placed in 300  $\mu\text{L}$  growth medium. Images of living cells were taken with a confocal microscope LSM 510 Meta (Zeiss, Germany). The laser lines used for excitation were 405 nm for DAPI, 488 nm for WGA488, and 543 nm for rhodamine.

**Magnetofection Experiments under Fluidic Conditions.** HeLa cells ( $10^5$ ) stably expressing the eGFP gene were seeded on a surface area of 250 mm<sup>2</sup> of a flow channel ( $\mu$ -Slide ibiTreat from Ibidi). According to the manufacturer, the seeding channel was treated to promote cell adhesion (ibiTreat). Prior to magnetofection, cells were allowed to grow overnight and were then cultured in Dulbecco's modified Eagle medium (DMEM) supplemented with additives and incubated at 37 °C in 5% CO<sub>2</sub> atmosphere. One hundred microliters of freshly prepared MAALs/siRNA<sup>Rh</sup> were injected into a reservoir containing 20 mL of cell medium. The reservoir containing MAALs/siRNA (rhodamine-labeled or unmodified) was connected to the cultured  $\mu$ -Slide I through a peristaltic pump. The velocity of the flow was regulated by the pump and set to 16 cm s<sup>-1</sup>. To allow magnetofection,

a cubic permanent magnet (NbFeB, 5 mm edge length, magnetic field strength of 1.3 T) was placed under the flow channel for 1 h while the flow was running. Images of the cells on the flow chamber, both at the region where the magnet was placed for magnetofection and at random regions of the rest of the chamber, were collected in 24 h time intervals with a fluorescence microscope AxioTech (Zeiss) which was equipped with phase contrast and two sets of green ( $\lambda_{\text{ex}} = 480 \text{ nm}$  and  $\lambda_{\text{em}} = 535 \text{ nm}$ , from AF Analysetechnik, Germany) and red ( $\lambda_{\text{ex}} = 530 \text{ nm}$  and  $\lambda_{\text{em}} = 615 \text{ nm}$ , from Zeiss) fluorescence filters. Illumination in transmission mode was provided by a 100 W white light source (halogen lamp, HAL-100 from Zeiss) whereas in fluorescence mode, illumination was provided by a HBO-100 lamp (from Zeiss). Unless otherwise specified, images were taken with an objective (Objective W "N-Achroplan" 20 $\times$ /0.5 M27) from Zeiss. Images were collected by a CCD camera (MRc AxioCam from Zeiss) connected to a PC and further analyzed with the software AxioVision (release 4.6 from Zeiss).

**Acknowledgment.** This work was supported by the BMBF/ERA-NET NEURON (project NanoSyn to W.J.P.) and by the Nanobiotechnology program (www.nanobio.de) of the German Federal Ministry of Education and Research (Grants 13N8186 and 13N8538 to C.P.). Financial support (to C.P.) from the German Excellence Initiative via the "Nanosystems Initiative Munich (NIM)" is also gratefully acknowledged.

**Supporting Information Available.** Complementary data corresponding to (i) incorporation of magnetic NPs to liposomes, (ii) characterization of MAALs/siRNA, (iii) additional data about cytotoxicity, (iv) MAALs/siRNA<sup>Rh</sup> uptake characterization by confocal microscopy and transmission electron microscopy, and (v) magnetofection under flow conditions. This material is available free of charge via the Internet at <http://pubs.acs.org>.

## REFERENCES AND NOTES

- Fire, A.; Xu, S.; Montgomery, M. K.; Kostas, S. A.; Driver, S. E.; Mello, C. C. *Nature* **1998**, *391*, 806–811.
- Elbashir, S. M.; Harborth, J.; Lendeckel, W.; Yalcin, A.; Weber, K.; Tuschl, T. *Nature* **2001**, *411*, 494–498.
- Juliano, R.; Alam, M. R.; Dixit, V.; Kang, H. *Nucleic Acids Res.* **2008**, *36*, 4158–4171.
- In Vivo RNAi: Performing RNAi Experiments in Animals; Ambion Applied Biosystems: Carlsbad, CA; [www.ambion.com/techlib/webcasts/siRNA0612.pdf](http://www.ambion.com/techlib/webcasts/siRNA0612.pdf).
- Munoz Javier, A.; del Pino, P.; Bedard, M. F.; Ho, D.; Skirtach, A. G.; Sukhorukov, G. B.; Plank, C.; Parak, W. J. *Langmuir* **2008**, *24*, 12517–12520.
- Rivera Gil, P.; De Koker, S.; De Geest, B. G.; Parak, W. J. *Nano Lett.* **2009**, *9*, 4398–4402.
- Nishiyama, N.; Kataoka, K. *Pharmacol. Ther.* **2006**, *112*, 630–648.
- Gary, D. J.; Puri, N.; Won, Y. J. *Controlled Release* **2007**, *121*, 64–73.
- Song, W.; Du, J.; Sun, T.; Zhang, P.; Wang, J. *Small* **2010**, *6*, 239–246.
- Patil, Y. B.; Swaminathan, S. K.; Sadhukha, T.; Ma, L.; Panyam, J. *Biomaterials* **2010**, *31*, 358–365.
- Tomar, R. S.; Matta, H.; Chaudhary, P. M. *Oncogene* **2003**, *22*, 5712–5715.

- (12) Qin, X.; An, D. S.; Chen, I. S.; Baltimore, D. *Proc. Natl. Acad. Sci. U.S.A.* **2003**, *100*, 183–188.
- (13) Pike-Overzet, K.; van der Burg, M.; Wagemaker, G.; van Dongen, J. J.; Staal, F. J. *Mol. Ther.* **2007**, *15*, 1910–1916.
- (14) Li, S.; Huang, L. *Gene Ther.* **2006**, *13*, 1313–1319.
- (15) Santel, A.; Aleku, M.; Keil, O.; Endruschat, J.; Esche, V.; Fisch, G.; Dames, S.; Löffler, K.; Fechtner, M.; Arnold, W.; Giese, K.; Klipfel, A.; Kaufmann, J. *Gene Ther.* **2006**, *13*, 1222–1234.
- (16) Schaffert, D.; Wagner, E. *Gene Ther.* **2008**, *15*, 1131–1138.
- (17) Zhou, J.; Wu, J.; Hafdi, N.; Behr, J.; Erbacher, P.; Peng, L. *Chem. Commun. (Cambridge, U.K.)* **2006**, 2362–2364.
- (18) Hornung, V.; Guenthner-Biller, M.; Bourquin, C.; Ablasser, A.; Schlee, M.; Uematsu, S.; Noronha, A.; Manoharan, M.; Akira, S.; de Fougerolles, A.; Endres, S.; Hartmann, G. *Nat. Med.* **2005**, *11*, 263–270.
- (19) Simeoni, F.; Morris, M. C.; Heitz, F.; Divita, G. *Nucleic Acids Res.* **2003**, *31*, 2717–2724.
- (20) Chu, T. C.; Twu, K. Y.; Ellington, A. D.; Levy, M. *Nucleic Acids Res.* **2006**, *34*, No. e73.
- (21) Giljohann, D. A.; Seferos, D. S.; Prigodich, A. E.; Patel, P. C.; Mirkin, C. A. *J. Am. Chem. Soc.* **2009**, *131*, 2072–2073.
- (22) Braun, G. B.; Pallaoro, A.; Wu, G.; Missirlis, D.; Zasadzinski, J. A.; Tirrell, M.; Reich, N. O. *ACS Nano* **2009**, *3*, 2007–2015.
- (23) Scherer, F.; Anton, M.; Schillinger, U.; Henke, J.; Bergemann, C.; Krüger, A.; Gänsbacher, B.; Plank, C. *Gene Ther.* **2002**, *9*, 102–109.
- (24) Plank, C.; Anton, M.; Rudolph, C.; Rosenecker, J.; Krötz, F. *Expert Opin. Biol. Ther.* **2003**, *3*, 745–758.
- (25) Plank, C.; Schillinger, U.; Scherer, F.; Bergemann, C.; Rémy, J.; Krötz, F.; Anton, M.; Lausier, J.; Rosenecker, J. *Biol. Chem.* **2003**, *384*, 737–747.
- (26) Unger, E. C.; McCreery, T. P.; Sweitzer, R. H.; Caldwell, V. E.; Wu, Y. *Invest. Radiol.* **1998**, *33*, 886–892.
- (27) Vlaskou, D.; Mykhaylyk, O.; Krötz, F.; Hellwig, N.; Renner, R.; Schillinger, U.; Gleich, B.; Rüger, A.; Schmitz, G.; Hensel, K.; Plank, C. *Adv. Funct. Mater.*, in press.
- (28) Djurovic, S.; Iversen, N.; Jeansson, S.; Hoover, F.; Christensen, G. *Mol. Biotechnol.* **2004**, *28*, 21–32.
- (29) Karmali, P. P.; Chaudhuri, A. *Med. Res. Rev.* **2007**, *27*, 696–722.
- (30) Akhtar, S.; Benter, I. F. *J. Clin. Invest.* **2007**, *117*, 3623–3632.
- (31) Mykhaylyk, O.; Antequera, Y. S.; Vlaskou, D.; Plank, C. *Nat. Protoc.* **2007**, *2*, 2391–2411.
- (32) Mykhaylyk, O.; Sánchez-Antequera, Y.; Vlaskou, D.; Hammerschmid, E.; Anton, M.; Zelphati, O.; Plank, C. *Methods Mol. Biol. (Totowa, NJ, U.S.)* **2010**, *605*, 487–525.
- (33) Hornung, V.; Guenthner-Biller, M.; Bourquin, C.; Ablasser, A.; Schlee, M.; Uematsu, S.; Noronha, A.; Manoharan, M.; Akira, S.; de Fougerolles, A.; Endres, S.; Hartmann, G. *Nat. Med.* **2005**, *11*, 263–270.
- (34) Fedorov, Y.; King, A.; Anderson, E.; Karpilow, J.; Ilsley, D.; Marshall, W.; Khvorova, A. *Nat. Methods* **2005**, *2*, 241.
- (35) Grimm, D.; Streetz, K. L.; Jopling, C. L.; Storm, T. A.; Pandey, K.; Davis, C. R.; Marion, P.; Salazar, F.; Kay, M. A. *Nature* **2006**, *441*, 537–541.
- (36) Zeblis, B.; Susha, A. S.; Sukhorukov, G. B.; Rogach, A. L.; Parak, W. J. *Langmuir* **2005**, *21*, 4262–4265.